ARCHIVES OF MECHANICS
Arch. Mech. **71** (4–5), 291–313, 2019, DOI: 10.24423/aom.3098

Computational method for shaping the vibro-isolation properties of semi-active and active systems

T. KRZYZYNSKI, I. MACIEJEWSKI

Department of Mechatronics and Applied Mechanics, Faculty of Technology and Education, Koszalin University of Technology, Śniadeckich 2, 75-453 Koszalin, Poland, e-mails: tomasz.krzyzynski@tu.koszalin.pl, igor.maciejewski@tu.koszalin.pl

The paper deals with an original methodology for modelling and control system design of the semi-active and active systems. At first a generalised simulation model of the vibration reduction system is formulated in such a way that it represents the dynamics of human body exposed to mechanical vibration. Then a novel control system design is proposed in order to adjust force characteristics of the fundamental elements included in the suspension system and consequently to reduce the harmful effects of vibration. Finally, a computational method is experimentally verified by selecting the vibro-isolation properties of an exemplary horizontal seat suspension for a specific input vibration.

Key words: vibration exposure, whole-body vibration.

Notation

$\mathbf{A}_{\mathrm{i}}$	state (system) matrix ($\mathrm{i} = x, y, z$),
$\mathbf{B}_{\mathrm{si}}$	input matrix corresponding to the excitation signal ($\mathrm{i} = x, y, z$),
$\mathbf{B}_{\mathrm{ai}}$	input matrix corresponding to the control signal ($\mathrm{i} = x, y, z$),
$\mathbf{C}_{\mathrm{i}}$	stiffness matrix of the bio-mechanical model of human body ($\mathrm{i} = x, y, z$),
$\mathbf{C}_{1\mathrm{i}}$, $\mathbf{C}_{2\mathrm{i}}$	output matrices ($\mathrm{i} = x, y, z$),
$\mathbf{D}_{\mathrm{i}}$	damping matrix of the bio-mechanical model of human body ($\mathrm{i} = x, y, z$),
$\mathbf{D}_{1\mathrm{si}}$, $\mathbf{D}_{2\mathrm{si}}$,	feedthrough (feedforward) matrices corresponding to the excitation signal ($\mathrm{i} = x, y, z$),
$\mathbf{D}_{1\mathrm{ai}}$, $\mathbf{D}_{2\mathrm{ai}}$	feedthrough (feedforward) matrices corresponding to the control signal ($\mathrm{i} = x, y, z$),
$\mathbf{K}_{\mathrm{i}}$	output feedback gain vector ($\mathrm{i} = x, y, z$),
$k_{1\mathrm{i}}$	control parameter corresponding to the relative displacement feedback loop ($\mathrm{i} = x, y, z$),
$k_{2\mathrm{i}}$	control parameter corresponding to the absolute velocity feedback loop ($\mathrm{i} = x, y, z$),
$\mathbf{F}_{\mathrm{ai}}$	vector of the active forces ($\mathrm{i} = x, y, z$),
$\mathbf{F}_{\mathrm{si}}$	vector of the exciting forces ($\mathrm{i} = x, y, z$),
F_{ai}	desired force of the actuator ($\mathrm{i} = x, y, z$), N,
$\mathbf{M}_{\mathrm{i}}$	inertia matrix of the bio-mechanical model of human body ($\mathrm{i} = x, y, z$),
$\mathbf{q}_{\mathrm{i}}$	displacement vector of the bio-mechanical model of human body ($\mathrm{i} = x, y, z$),

q_{1i} displacement of the isolated body for the selected direction of the vibration exposure ($\mathrm{i} = x, y, z$), m,
q_{si} displacement of the input vibration ($\mathrm{i} = x, y, z$), m,
s_{ti} suspension travel for the selected direction of the vibration exposure ($\mathrm{i} = x, y, z$), m,
$\mathrm{TFE_i}$ frequency weighted transmissibility factor for the selected direction of the vibration exposure ($\mathrm{i} = x, y, z$),
u_i control signal ($\mathrm{i} = x, y, z$), V,
$\mathbf{w}_{si}$ vector of the external disturbances ($\mathrm{i} = x, y, z$),
$\mathbf{x}_d$ vector of the selected decision variables,
$\mathbf{x}_i$ state vector ($\mathrm{i} = x, y, z$),
$\mathbf{y}_i$ measurement vector ($\mathrm{i} = x, y, z$),
$\mathbf{z}_i$ output vector ($\mathrm{i} = x, y, z$).

1. Introduction

Passive vibration reduction systems are commonly assembled by utilising inertial and visco-elastic elements. Even though they dissipate a considerable portion of the oscillation energy over a higher range of frequencies, large amplitude oscillations are amplified at the system's resonant frequencies [1]. As a result, it is difficult to absorb vibration energy when the frequency of its oscillations matches the system's natural frequency [2]. Therefore semi-active or active suspension systems have to be employed for the purpose of increasing the vibration damping effectiveness [3].

Unluckily, the dynamic characteristics of most actuators are modelled as strongly non-linear functions due to the system constraints and its design requirements. Thus, the advanced control strategy has to take into account the non-linear modelling of such actuators as well as their time variation behaviour. Nowadays, different kinds of non-linear drives (e.g. pneumatic, hydraulic, electromagnetic) are employed as the force generators for attenuating shock and vibration inputs transmitted to the human body [4]. There are several methods of the semi-active and active vibration control including sliding-mode control [5], adaptive robust control [6] or fuzzy logic control [7]. Nevertheless, it is not acknowledged how to predict and adapt the desired active force for various working conditions. There is a lack of sophisticated procedures for control synthesis and selecting the optimal control parameters if the vibration reduction systems are described by non-linear equations of motion.

In the paper a complex method for shaping the vibro-isolation properties of semi-active and active systems is proposed in order to obtain an optimal vibration isolation of the human body. The feedback control of the vibration reduction system is intended to improve its dynamics and shape the system characteristics especially for a specific vibro-isolation process (Fig. 1). A linear state-feedback control law is applied in order to evaluate the desired active force by means of the primary controller. However, the feedback gains are calculated

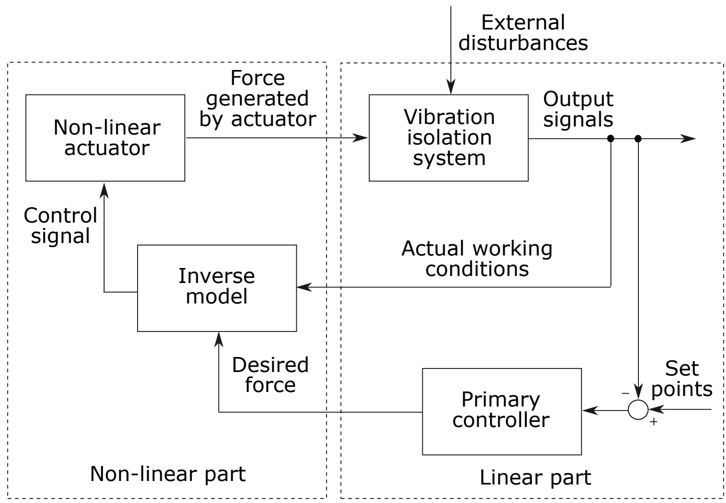

FIG. 1. Block diagram of the overall control structure of vibration reduction systems.

by using the Pareto-optimal approach unlike in conventional control methods. For instance, the Linear-Quadratic (LQ) control theory [8] is often employed for determining the optimal control to minimise a performance index of suspension systems. The LQ control can be used in the initial design process to obtain the global overview of all possible optimal solutions for the selected trade-off between regulation performance and the control effort. Further search of the best solution is possible using a computational method proposed in this paper, which can accept the vibro-isolation criteria representing the varied sensitivity of the human body in different frequency ranges.

The H-inf control is intensively discussed these days in the context of robustness and disturbance attenuation of the semi-active or active suspension systems [9, 10]. The paper [9] clearly shows that H-inf control effectively deals with the conflicted suspension performance problem by using a multi-objective functional. Two main performance requirements are normally considered for the advanced seat suspension systems, i.e. ride comfort and suspension deflection. It is established in the H-inf framework to use weighting functions in order to shape a proper compromise between these conflicted requirements, however the robust H-inf control is applicable for uncertain linear systems. The paper [10] presents a robust output feedback control design for an active suspension system considering uncertain driver's biodynamics. A specific model of the seated human body under vertical vibration is considered as well as in many other studies, while in this paper a generalised methodology for modelling and the control system design is proposed. Unlike in existing papers a lumped parameter model of the human body model may be adopted for different directions of the vibration transmission.

Assuming that the desired force is determined by the primary controller, then such a force has to be reproduced by the semi-active or active actuator of non-linear characteristics (Fig. 1). This can be achieved by using the force tracking control system that adjusts controllable drive. Typically, the force tracking control system is handled by applying an internal force feedback [11]. Differently from conventional force control techniques, in this paper an inverse model of the control element has to be calculated instead of applying any force feedback. A specific force characteristics of the chosen actuator and its parameters should be evaluated experimentally in order to get a high compatibility between the model and reality. If some model parameters are not well-defined, the lower agreement between the desired force and the actual actuator force can be obtained. Therefore, the proposed computational method works properly when a reliable model of the force actuator is created.

Such a proposed control system allows shaping vibro-isolation properties of the system for the specified excitation signals and different working conditions. Using a unique vibration control system, whose structure and individual components are proposed in this paper, it is possible to find a set of the compromising system configurations (Pareto-optimal solutions) that are selected by suitable changing of the control parameters.

2. Overall configuration of the proposed methodology

The block diagram for an overall configuration of the proposed methodology is shown in Fig. 2. At the beginning, random input signal must be generated in order to reproduce vibration occurring in a specific working machine. Then the dynamical behaviour of vibration reduction system has to be numerically simulated in the interest of shaping the vibro-isolation properties of semi-active as well as active systems. Output signals of the simulation model are required for the

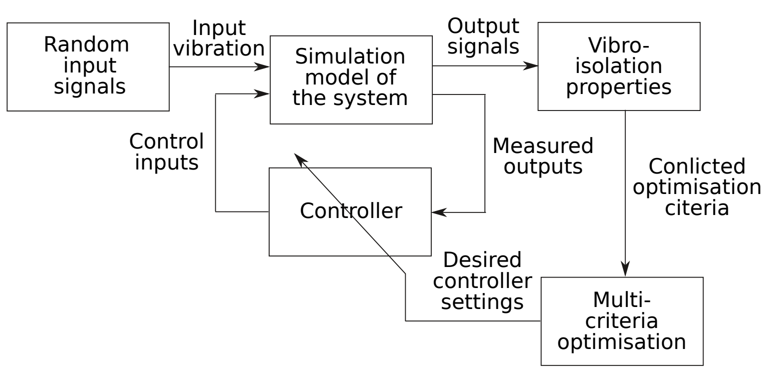

Fig. 2. Block diagram of the computational method for shaping vibro-isolation properties.

sake of evaluating the risks to health from whole-body vibration. Subsequently, multi-criteria optimisation is used for determining the control parameters that provide the best system performance in view of the conflicted requirements for modern suspensions.

3. Simulation model of the vibration reduction system

In this paper the computational model of the vibration reduction system is required for the purpose of simulating its dynamic response under various input vibrations. An accurate prediction of the system dynamics is extremely helpful for designing a controller and it supports further optimising of its parameters.

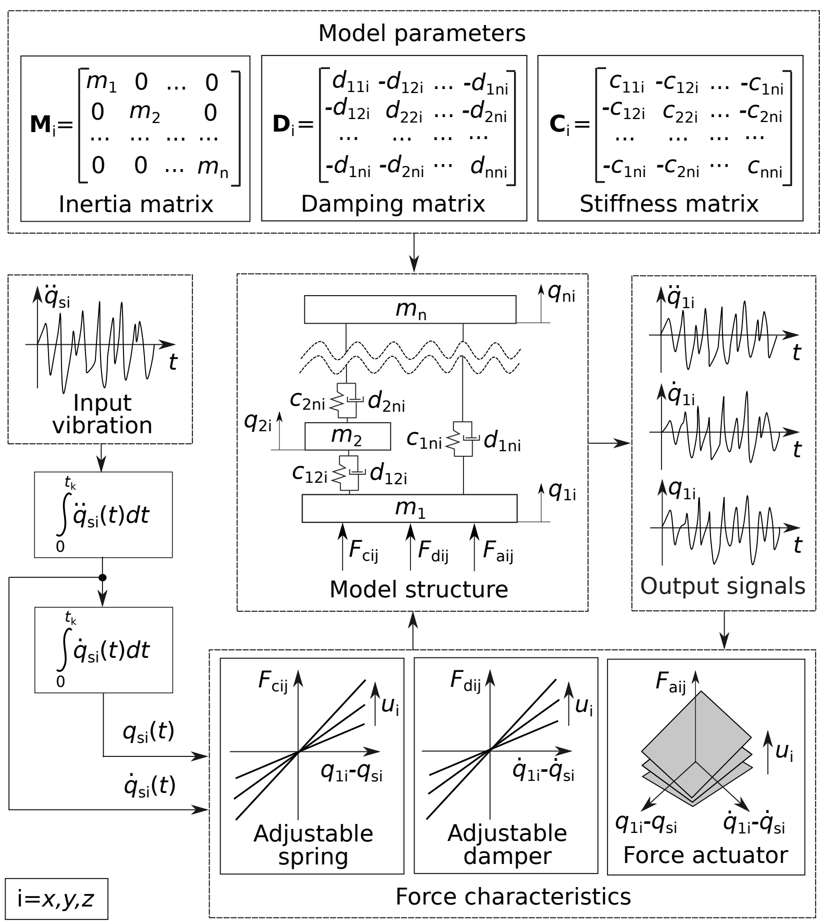

Fig. 3. Block diagram for numerical simulation of the dynamic behaviour of vibration reduction systems.

In order to prepare such a complex simulation model, the system modelling equations have to be combined together with the complete control strategy for the purpose of studying the closed-loop behavior at different values of the control parameters. A generalised simulation model of the semi-active or active vibration reduction system is shown in Fig. 3.

Firstly, the input vibration block (Fig. 3) should be created due to necessity of generating the random acceleration $\ddot{q}_{\mathrm{si}}(t)$ for a specific direction of the vibration exposure ($\mathrm{i} = x, y, z$). Such an acceleration signal must be integrated twice over time to calculate the velocity $\dot{q}_{\mathrm{si}}(t)$ and displacement $q_{\mathrm{si}}(t)$ that are required as input signals to the simulation model. The forces of adjustable spring F_{cij}, adjustable damper F_{dij} or force actuator F_{aij} are used to protect the human body against unhealthy vibrations. The force characteristics of such controllable elements have to be determined for a unique system solution of the semi-active or active suspension as non-linear functions of the input signal u_{i} and the system relative displacement $q_{1\mathrm{i}} - q_{\mathrm{si}}$ and/or relative velocity $\dot{q}_{1\mathrm{i}} - \dot{q}_{\mathrm{si}}$.

Secondly, a model structure describing the human body dynamics must be defined in the basis of well-known bio-mechanical models [12–14]. Their equations of motion shall be expressed for a single-axis ($\mathrm{i} = x, y, z$) of the vibration exposure as follows:

$$\mathbf{M}_{\mathrm{i}}\ddot{\mathbf{q}}_{\mathrm{i}} + \mathbf{D}_{\mathrm{i}}\dot{\mathbf{q}}_{\mathrm{i}} + \mathbf{C}_{\mathrm{i}}\mathbf{q}_{\mathrm{i}} = -\mathbf{F}_{\mathrm{si}} + \mathbf{F}_{\mathrm{ai}}, \qquad \mathrm{i} = x, y, z \tag{3.1}$$

where: $\mathbf{q}_{\mathrm{i}}$ is the vector of isolated body displacements, $\mathbf{M}_{\mathrm{i}}$ is the inertia matrix, $\mathbf{D}_{\mathrm{i}}$ is the damping matrix, $\mathbf{C}_{\mathrm{i}}$ is the stiffness matrix, $\mathbf{F}_{\mathrm{si}}$ is the vector containing exciting forces and $\mathbf{F}_{\mathrm{ai}}$ is the vector of forces applied actively.

The inertia matrix $\mathbf{M}_{\mathrm{i}}$ is a diagonal matrix (size $n \times n$) and it designates particular masses included in the chosen bio-mechanical model of human body:

$$\mathbf{M}_{\mathrm{i}} = \begin{bmatrix} m_1 & 0 & 0 & \cdots & 0 \\ 0 & m_2 & 0 & \cdots & 0 \\ 0 & 0 & m_3 & \cdots & 0 \\ \cdots & \cdots & \cdots & \ddots & \cdots \\ 0 & 0 & 0 & \ldots & m_{\mathrm{n}} \end{bmatrix}. \tag{3.2}$$

The damping matrix $\mathbf{D}_{\mathrm{i}}$ is a symmetric matrix (size $n \times n$) and must be specified for a single-axis ($\mathrm{i} = x, y, z$) of the vibration transmission:

$$\mathbf{D}_{\mathrm{i}} = \begin{bmatrix} d_{11\mathrm{i}} & -d_{12\mathrm{i}} & -d_{13\mathrm{i}} & \cdots & -d_{1\mathrm{ni}} \\ -d_{12\mathrm{i}} & d_{22\mathrm{i}} & -d_{23\mathrm{i}} & \cdots & -d_{2\mathrm{ni}} \\ -d_{13\mathrm{i}} & -d_{23\mathrm{i}} & d_{33\mathrm{i}} & \cdots & -d_{3\mathrm{ni}} \\ \cdots & \cdots & \cdots & \ddots & \cdots \\ -d_{1\mathrm{ni}} & -d_{2\mathrm{ni}} & -d_{3\mathrm{ni}} & \ldots & d_{\mathrm{nni}} \end{bmatrix}, \quad \mathrm{i} = x, y, z, \tag{3.3}$$

where the individual elements appearing on the principal diagonal are calculated as follows:

$$
\begin{aligned}
&d_{11\mathrm{i}} = d_{1\mathrm{i}} + d_{12\mathrm{i}} + d_{13\mathrm{i}} + \cdots + d_{1\mathrm{ni}},\\
&d_{22\mathrm{i}} = d_{2\mathrm{i}} + d_{12\mathrm{i}} + d_{23\mathrm{i}} + \cdots + d_{2\mathrm{ni}},\\
&d_{33\mathrm{i}} = d_{3\mathrm{i}} + d_{13\mathrm{i}} + d_{23\mathrm{i}} + \cdots + d_{3\mathrm{ni}}, \qquad \mathrm{i} = x, y, z.\\
&\ldots\\
&d_{\mathrm{nni}} = d_{\mathrm{ni}} + d_{1\mathrm{ni}} + d_{2\mathrm{ni}} + \cdots + d_{(\mathrm{n}-1)\mathrm{ni}},
\end{aligned}
\tag{3.4}
$$

The stiffness matrix $\mathbf{C}_\mathrm{i}$ is also symmetric (size $n \times n$) and should be delivered in the following form:

$$
\mathbf{C}_\mathrm{i} = \begin{bmatrix}
c_{11\mathrm{i}} & -c_{12\mathrm{i}} & -c_{13\mathrm{i}} & \cdots & -c_{1\mathrm{ni}}\\
-c_{12\mathrm{i}} & c_{22\mathrm{i}} & -c_{23\mathrm{i}} & \cdots & -c_{2\mathrm{ni}}\\
-c_{13\mathrm{i}} & -c_{23\mathrm{i}} & c_{33\mathrm{i}} & \cdots & -c_{3\mathrm{ni}}\\
\ldots & \ldots & \ldots & \ddots & \ldots\\
-c_{1\mathrm{ni}} & -c_{2\mathrm{ni}} & -c_{3\mathrm{ni}} & \ldots & c_{\mathrm{nni}}
\end{bmatrix}, \quad \mathrm{i} = x, y, z,
\tag{3.5}
$$

together with the following elements that are located on its principal diagonal:

$$
\begin{aligned}
&c_{11\mathrm{i}} = c_{1\mathrm{i}} + c_{12\mathrm{i}} + c_{13\mathrm{i}} + \cdots + c_{1\mathrm{ni}},\\
&c_{22\mathrm{i}} = c_{2\mathrm{i}} + c_{12\mathrm{i}} + c_{23\mathrm{i}} + \cdots + c_{2\mathrm{ni}},\\
&c_{33\mathrm{i}} = c_{3\mathrm{i}} + c_{13\mathrm{i}} + c_{23\mathrm{i}} + \cdots + c_{3\mathrm{ni}}, \qquad \mathrm{i} = x, y, z.\\
&\ldots\\
&c_{\mathrm{nni}} = c_{\mathrm{ni}} + c_{1\mathrm{ni}} + c_{2\mathrm{ni}} + \cdots + c_{(\mathrm{n}-1)\mathrm{ni}},
\end{aligned}
\tag{3.6}
$$

A suitable choice of the individual values of masses $m_1, m_2, \ldots, m_\mathrm{n}$, damping $d_{11\mathrm{i}}, d_{12\mathrm{i}}, \ldots, d_{\mathrm{nni}}$ and stiffness $c_{11\mathrm{i}}, c_{12\mathrm{i}}, \ldots, c_{\mathrm{nni}}$ coefficients allows to reflect the human dynamics exposed to whole-body vibrations, and thus to calculate the displacements $q_{1\mathrm{i}}, q_{2\mathrm{i}}, \ldots, q_{\mathrm{ni}}$ of particular bodies included in the model. The output acceleration $\ddot{q}_{1\mathrm{i}}(t)$ is necessary for measuring the human exposure to vibration, while the output velocity $\dot{q}_{1\mathrm{i}}(t)$ and output displacement $q_{1\mathrm{i}}(t)$ are required for vibration control by using the adjustable spring, adjustable damper or force actuator.

4. Vibration control system

The control system synthesis is performed on the basis of a generalised model of the hybrid suspension that is shown in Fig. 4. Such a model is intensely discussed in the modern literature because it captures the essential dynamical properties of different suspension systems [15, 16]. The damping $d_{11\mathrm{i}}, d_{12\mathrm{i}}, \ldots, d_{\mathrm{nni}}$ and stiffness $c_{11\mathrm{i}}, c_{12\mathrm{i}}, \ldots, c_{\mathrm{nni}}$ coefficients correspond to the human body part moving free without any support (for example head movements), while the damping

$d_{1\mathrm{i}}, d_{2\mathrm{i}}, \ldots, d_{\mathrm{ni}}$ and stiffness $c_{1\mathrm{i}}, c_{2\mathrm{i}}, \ldots, c_{\mathrm{ni}}$ coefficients (Fig. 4) represent the reaction of the human body to immovable elements in the vehicle (for example hands on the steering wheel).

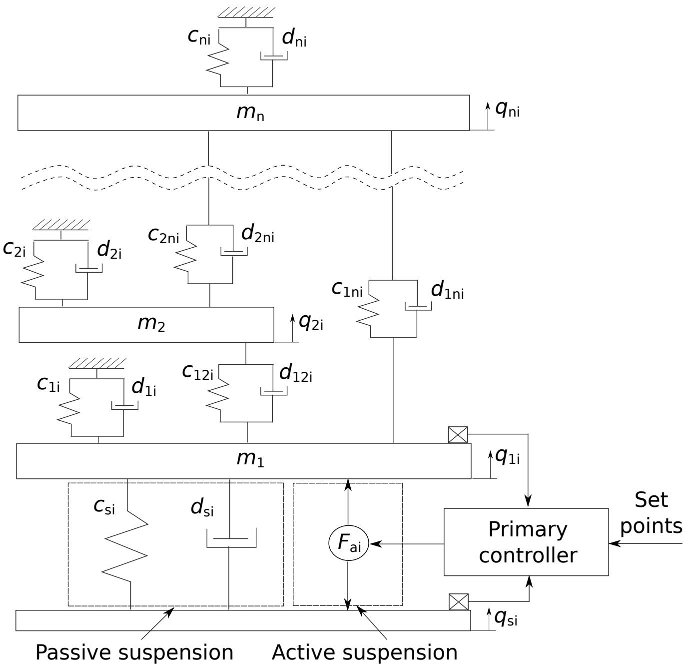

Fig. 4. Generalised model of the hybrid vibration reduction system for one direction of the vibration transmission ($\mathrm{i} = x, y, z$).

In order to depict a movement of this system, the following state variables are chosen:

$$\mathbf{x}_{\mathrm{i}}(t) := [q_{1\mathrm{i}}, \dot{q}_{1\mathrm{i}}, q_{2\mathrm{i}}, \dot{q}_{2\mathrm{i}}, \ldots, q_{\mathrm{ni}}, \dot{q}_{\mathrm{ni}}]^{\mathrm{T}}, \qquad \mathrm{i} = x, y, z \tag{4.1}$$

where $q_{1\mathrm{i}}, q_{2\mathrm{i}}, \ldots, q_{\mathrm{ni}}$ are the displacements of the particular elements contained in the bio-mechanical model of human body (Fig. 4) and $\dot{q}_{1\mathrm{i}}, \dot{q}_{2\mathrm{i}}, \ldots, \dot{q}_{\mathrm{ni}}$ are the corresponding velocities.

The external disturbances interfere with a proper functioning of the controlled system and they are included in the model as follows:

$$\mathbf{w}_{\mathrm{si}}(t) := [q_{\mathrm{si}}, \dot{q}_{\mathrm{si}}]^{\mathrm{T}}, \qquad \mathrm{i} = x, y, z \tag{4.2}$$

where q_{si} and $\dot{q}_{\mathrm{si}}$ are the displacement and the velocity of input vibration, respectively.

The state-space equation of hybrid vibration reduction system is then achieved by employing the Linear Fractional Transformation (LFT) technique [17] in the following manner:

$$\dot{\mathbf{x}}_\mathrm{i}(t) = \mathbf{A}_\mathrm{i}\mathbf{x}_\mathrm{i}(t) + \mathbf{B}_\mathrm{si}\mathbf{w}_\mathrm{si}(t) + \mathbf{B}_\mathrm{ai}F_\mathrm{ai}(t), \qquad \mathrm{i} = x, y, z \tag{4.3}$$

where: F_ai is the force that should be provided into the system actively for the sake of reducing harmful vibrations.

The state (system) matrix is given in the following configuration:

$$\mathbf{A}_\mathrm{i} = \begin{bmatrix} 0 & 1 & 0 & 0 & \cdots & 0 & 0 \\ -\frac{c_\mathrm{11i}}{m_1} & -\frac{d_\mathrm{11i}}{m_1} & \frac{c_\mathrm{12i}}{m_1} & \frac{d_\mathrm{12i}}{m_1} & \cdots & \frac{c_\mathrm{1ni}}{m_1} & \frac{d_\mathrm{1ni}}{m_1} \\ 0 & 0 & 0 & 1 & \cdots & 0 & 0 \\ \frac{c_\mathrm{12i}}{m_2} & \frac{d_\mathrm{12i}}{m_2} & -\frac{c_\mathrm{22i}}{m_2} & -\frac{d_\mathrm{22i}}{m_2} & \cdots & \frac{c_\mathrm{2ni}}{m_2} & \frac{d_\mathrm{2ni}}{m_2} \\ \cdots & \cdots & \cdots & \cdots & \cdots & \cdots & \cdots \\ 0 & 0 & 0 & 0 & \cdots & 0 & 1 \\ \frac{c_\mathrm{1ni}}{m_\mathrm{n}} & \frac{d_\mathrm{1ni}}{m_\mathrm{n}} & \frac{c_\mathrm{2ni}}{m_\mathrm{n}} & \frac{d_\mathrm{2ni}}{m_\mathrm{n}} & \cdots & -\frac{c_\mathrm{nni}}{m_\mathrm{n}} & -\frac{d_\mathrm{nni}}{m_\mathrm{n}} \end{bmatrix}. \tag{4.4}$$

The selected damping $d_\mathrm{11i}, d_\mathrm{22i}, \ldots, d_\mathrm{nni}$ and stiffness $c_\mathrm{11i}, c_\mathrm{22i}, \ldots, c_\mathrm{nni}$ coefficients should be calculated according to Eqs. (3.4) and (3.6).

The input matrices are defined utilising the following structure:

$$\mathbf{B}_\mathrm{si} = \begin{bmatrix} 0 & 0 \\ \frac{c_\mathrm{si}}{m_1} & \frac{d_\mathrm{si}}{m_1} \\ 0 & 0 \\ 0 & 0 \\ \cdots & \cdots \\ 0 & 0 \\ 0 & 0 \end{bmatrix}, \qquad \mathbf{B}_\mathrm{ai} = \begin{bmatrix} 0 \\ \frac{1}{m_1} \\ 0 \\ 0 \\ \cdots \\ 0 \\ 0 \end{bmatrix}. \tag{4.5}$$

In turn, the acceleration $\ddot{q}_\mathrm{1i}$ of a suspended body and the relative displacement $q_\mathrm{1i} - q_\mathrm{si}$ of the suspension system are designated as the output variables, therefore the output vector is given as follows:

$$\mathbf{z}_\mathrm{i}(t) := [\ddot{q}_\mathrm{1i}, q_\mathrm{1i} - q_\mathrm{si}]^\mathrm{T}, \qquad \mathrm{i} = x, y, z. \tag{4.6}$$

Then, the output equation should be defined as:

$$\mathbf{z}_\mathrm{i}(t) = \mathbf{C}_\mathrm{1i}\mathbf{x}_\mathrm{i}(t) + \mathbf{D}_\mathrm{1si}\mathbf{w}_\mathrm{si}(t) + \mathbf{D}_\mathrm{1ai}F_\mathrm{ai}(t), \qquad \mathrm{i} = x, y, z \tag{4.7}$$

together with the related output matrix:

$$\mathbf{C}_\mathrm{1i} = \begin{bmatrix} -\frac{c_\mathrm{11i}}{m_1} & -\frac{d_\mathrm{11i}}{m_1} & \frac{c_\mathrm{12i}}{m_1} & \frac{d_\mathrm{12i}}{m_1} & \cdots & \frac{c_\mathrm{1ni}}{m_1} & \frac{d_\mathrm{1ni}}{m_1} \\ 1 & 0 & 0 & 0 & \cdots & 0 & 0 \end{bmatrix}. \tag{4.8}$$

The feedforward matrices are determined by using the subsequent formula:

$$\mathbf{D}_{1\mathrm{si}} = \begin{bmatrix} \frac{c_{\mathrm{si}}}{m_1} & \frac{d_{\mathrm{si}}}{m_1} \\ -1 & 0 \end{bmatrix}, \qquad \mathbf{D}_{1\mathrm{ai}} = \begin{bmatrix} \frac{1}{m_1} \\ 0 \end{bmatrix}. \tag{4.9}$$

The relative displacement $q_{1\mathrm{i}} - q_{\mathrm{si}}$ of the suspension system and the absolute velocity $\dot{q}_{1\mathrm{i}}$ of a suspended body are required to be measurable. There are many high-resolution sensors available on the market that are used for distance and position measurements. Accelerometers are most commonly used to measure vibration, however an acceleration signal has to be integrated in order to obtain the velocity signal. In practice the integration of an acceleration signal shall be realized simultaneously with high-pass filtering to prevent spurious offsets, drifts, etc. Hence the measurement vector can be successfully presented in the following form:

$$\mathbf{y}_{\mathrm{i}}(t) := [q_{1\mathrm{i}} - q_{\mathrm{si}}, \dot{q}_{1\mathrm{i}}]^{\mathrm{T}}, \qquad \mathrm{i} = x, y, z. \tag{4.10}$$

Consequently, the measurement equation is formulated in the following manner:

$$\mathbf{y}_{\mathrm{i}}(t) = \mathbf{C}_{2\mathrm{i}}\mathbf{x}_{\mathrm{i}}(t) + \mathbf{D}_{2\mathrm{si}}\mathbf{w}_{\mathrm{si}}(t) + \mathbf{D}_{2\mathrm{ai}}F_{\mathrm{ai}}(t), \qquad \mathrm{i} = x, y, z \tag{4.11}$$

together with the corresponding matrices:

$$\mathbf{C}_{2\mathrm{i}} = \begin{bmatrix} 1 & 0 & 0 & 0 & \cdots & 0 & 0 \\ 0 & 1 & 0 & 0 & \cdots & 0 & 0 \end{bmatrix}, \tag{4.12}$$

$$\mathbf{D}_{2\mathrm{si}} = \begin{bmatrix} -1 & 0 \\ 0 & 0 \end{bmatrix}, \qquad \mathbf{D}_{2\mathrm{ai}} = \begin{bmatrix} 0 \\ 0 \end{bmatrix}. \tag{4.13}$$

As follows from Eq. (4.11), the state feedback control problem is solved by utilising the following regulation strategy of the suspension system:

$$F_{\mathrm{ai}}(t) = \mathbf{K}_{\mathrm{i}}\mathbf{y}_{\mathrm{i}}(t), \qquad \mathrm{i} = x, y, z \tag{4.14}$$

where: $\mathbf{K}_{\mathrm{i}} = [k_{1\mathrm{i}}, k_{2\mathrm{i}}]$ is the output feedback gain vector to be designed especially for a specific input vibration. Although the proposed control strategy (Eq. (4.14)) does not take into account the limited suspension displacement, further in this paper the multi-criteria optimisation is employed in order to select such values of the control parameters which prevent end-stop impacts caused by the large amplitudes of the input vibration.

In this paper it is suggested to reproduce the desired active force F_{ai} by using the inverse model of a specific control element. Current values of the control signal u_{i} shall be calculated regarding to an unique control strategy that includes the following elements:

• adjustable spring

$$u_{\mathrm{i}} = \begin{cases} f(q_{1\mathrm{i}} - q_{\mathrm{si}}, F_{\mathrm{ai}}) & \text{for } F_{\mathrm{ai}}(q_{1\mathrm{i}} - q_{\mathrm{si}}) > 0, \\ 0 & \text{for } F_{\mathrm{ai}}(q_{1\mathrm{i}} - q_{\mathrm{si}}) \leq 0; \end{cases} \tag{4.15}$$

• adjustable damper

$$u_{\mathrm{i}} = \begin{cases} f(\dot{q}_{1\mathrm{i}} - \dot{q}_{\mathrm{si}}, F_{\mathrm{ai}}) & \text{for } F_{\mathrm{ai}}(\dot{q}_{1\mathrm{i}} - \dot{q}_{\mathrm{si}}) > 0, \\ 0 & \text{for } F_{\mathrm{ai}}(\dot{q}_{1\mathrm{i}} - \dot{q}_{\mathrm{si}}) \leq 0; \end{cases} \tag{4.16}$$

• force actuator

$$u_{\mathrm{i}} = f(q_{1\mathrm{i}} - q_{\mathrm{si}}, \dot{q}_{1\mathrm{i}} - \dot{q}_{\mathrm{si}}, F_{\mathrm{ai}}) \tag{4.17}$$

where $q_{1\mathrm{i}} - q_{\mathrm{si}}$ and $\dot{q}_{1\mathrm{i}} - \dot{q}_{\mathrm{si}}$ are the signals taking into account the actual working conditions of particular control elements for the different directions of the vibration exposure ($\mathrm{i} = x, y, z$).

5. Example: Control synthesis of the horizontal suspension system with seated human body

5.1. Physical and mathematical model of the system

An exemplary seat suspension system, that is under investigation in the following paper, is shown in Fig. 5. In this system a simplified model of the human body is utilised for reproducing its biodynamic response in the horizontal x-direction of the vibration exposure [13]. The human subject is represented as a 3-DOF lumped parameter model with three interconnected masses by using linear springs and dampers. The first mass corresponds to the seat upper part frame (m_1), while the subsequent masses represent the sitting part of the human body (m_2) in contact with the back support and the sitting part of the human body (m_3) not in contact with the back support. The equivalent stiffness

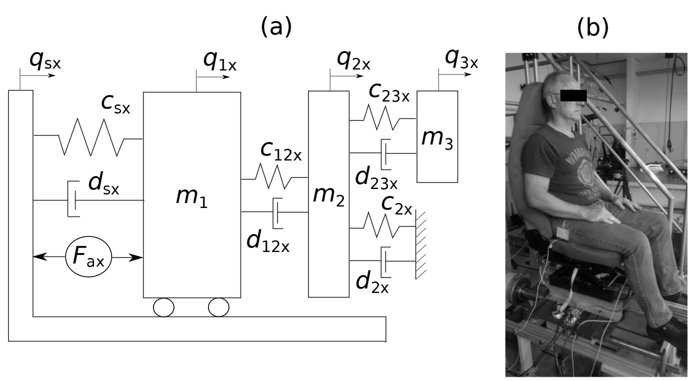

Fig. 5. Physical model of the active horizontal seat suspension with seated human body (a) and laboratory experimental set-up (b).

$c_{12\mathrm{x}}$ and damping $d_{12\mathrm{x}}$ coefficients describe visco-elastic properties of the human body part in contact with the back cushion. In turn, the coefficients $c_{2\mathrm{x}}$ and $d_{2\mathrm{x}}$ characterize the reactions exerted by hands on the steering wheel while the coefficients $c_{23\mathrm{x}}$ and $d_{23\mathrm{x}}$ define the head movements that are carried out without the back support. The kinematic excitation q_{sx} is applied in order to generate mechanical vibration of the modelled structure.

To calculate the desired force F_{ax} that have to be introduced into the system actively, the linear spring c_{sx} and linear damper d_{sx} are used for the purpose of reproducing the general dynamic properties of the suspension system. Such a linear suspension system may be described by employing a state space representation, thus the following state variables are chosen to express the human body movement in response to mechanical vibration:

$$\mathbf{x}_{\mathrm{x}}(t) := [q_{1\mathrm{x}}, \dot{q}_{1\mathrm{x}}, q_{2\mathrm{x}}, \dot{q}_{2\mathrm{x}}, q_{3\mathrm{x}}, \dot{q}_{3\mathrm{x}}]^{\mathrm{T}} \tag{5.1}$$

where $q_{1\mathrm{x}}, q_{2\mathrm{x}}, q_{3\mathrm{x}}$ and $\dot{q}_{1\mathrm{x}}, \dot{q}_{2\mathrm{s}}, \dot{q}_{3\mathrm{x}}$ are the corresponding displacements and velocities of the human body model (Fig. 5a). The displacement q_{sx} and velocity $\dot{q}_{\mathrm{sx}}$ of the input vibration are selected as the external disturbances that affect a proper functioning of the modelled system:

$$\mathbf{w}_{\mathrm{sx}}(t) := [q_{\mathrm{sx}}, \dot{q}_{\mathrm{sx}}]^{\mathrm{T}}. \tag{5.2}$$

A state-space equation of the system is achieved by considering the active force F_{ax} to be introduced into the system as an output from a controller:

$$\dot{\mathbf{x}}_{\mathrm{x}}(t) = \mathbf{A}_{\mathrm{x}}\mathbf{x}_{\mathrm{x}}(t) + \mathbf{B}_{\mathrm{sx}}\mathbf{w}_{\mathrm{sx}}(t) + \mathbf{B}_{\mathrm{ax}}F_{\mathrm{ax}}(t). \tag{5.3}$$

The state (system) matrix is presented as the succeeding expression:

$$\mathbf{A}_{\mathrm{x}} = \begin{bmatrix} 0 & 1 & 0 & 0 & 0 & 0 \\ -\frac{c_{11\mathrm{x}}}{m_1} & -\frac{d_{11\mathrm{x}}}{m_1} & \frac{c_{12\mathrm{x}}}{m_1} & \frac{d_{12\mathrm{x}}}{m_1} & 0 & 0 \\ 0 & 0 & 0 & 1 & 0 & 0 \\ \frac{c_{12\mathrm{x}}}{m_2} & \frac{d_{12\mathrm{x}}}{m_2} & -\frac{c_{22\mathrm{x}}}{m_2} & -\frac{d_{22\mathrm{x}}}{m_2} & \frac{c_{2\mathrm{ni}}}{m_2} & \frac{d_{2\mathrm{ni}}}{m_2} \\ 0 & 0 & 0 & 0 & 0 & 1 \\ 0 & 0 & \frac{c_{23\mathrm{x}}}{m_3} & \frac{d_{23\mathrm{x}}}{m_3} & -\frac{c_{33\mathrm{x}}}{m_3} & -\frac{d_{33\mathrm{x}}}{m_3} \end{bmatrix}. \tag{5.4}$$

Than, the input matrices take the following form:

$$\mathbf{B}_{\mathrm{sx}} = \begin{bmatrix} 0 & 0 \\ \frac{c_{\mathrm{sx}}}{m_1} & \frac{d_{\mathrm{sx}}}{m_1} \\ 0 & 0 \\ 0 & 0 \\ 0 & 0 \\ 0 & 0 \end{bmatrix}, \qquad \mathbf{B}_{\mathrm{ax}} = \begin{bmatrix} 0 \\ \frac{1}{m_1} \\ 0 \\ 0 \\ 0 \\ 0 \end{bmatrix}. \tag{5.5}$$

The following damping $d_{11\mathrm{x}}, d_{22\mathrm{x}}, d_{33\mathrm{x}}$ and stiffness $c_{11\mathrm{x}}, c_{22\mathrm{x}}, c_{33\mathrm{x}}$ coefficients are determined with the assistance of further relationships:

$$
\begin{aligned}
&d_{11\mathrm{x}} = d_{12\mathrm{x}} + d_{\mathrm{sx}}, && c_{11\mathrm{x}} = c_{12\mathrm{x}} + c_{\mathrm{sx}},\\
&d_{22\mathrm{x}} = d_{2\mathrm{x}} + d_{12\mathrm{x}} + d_{23\mathrm{x}}, && c_{22\mathrm{x}} = c_{2\mathrm{x}} + c_{12\mathrm{x}} + c_{23\mathrm{x}},\\
&d_{33\mathrm{x}} = d_{23\mathrm{x}}, && c_{33\mathrm{x}} = c_{23\mathrm{x}}.
\end{aligned}
\tag{5.6}
$$

In order to control the vibration damping effectiveness, the suspended body acceleration $\ddot{q}_{1\mathrm{x}}$ and the relative displacement $q_{1\mathrm{x}} - q_{\mathrm{sx}}$ of the suspension system are selected, hence the output vector is defined as:

$$
\mathbf{z}_{\mathrm{x}}(t) := [\ddot{q}_{1\mathrm{x}}, q_{1\mathrm{x}} - q_{\mathrm{sx}}]^{\mathrm{T}}. \tag{5.7}
$$

Consequently, the output equation is formulated in the following way:

$$
\mathbf{z}_{\mathrm{x}}(t) = \mathbf{C}_{1\mathrm{x}}\mathbf{x}_{\mathrm{x}}(t) + \mathbf{D}_{1\mathrm{sx}}\mathbf{w}_{\mathrm{sx}}(t) + \mathbf{D}_{1\mathrm{ax}}F_{\mathrm{ax}}(t) \tag{5.8}
$$

together with the following output matrix:

$$
\mathbf{C}_{1\mathrm{x}} = \begin{bmatrix} -\frac{c_{11\mathrm{x}}}{m_1} & -\frac{d_{11\mathrm{x}}}{m_1} & \frac{c_{12\mathrm{x}}}{m_1} & \frac{d_{12\mathrm{x}}}{m_1} & 0 & 0\\ 1 & 0 & 0 & 0 & 0 & 0 \end{bmatrix}. \tag{5.9}
$$

Successively, the feedforward matrices are supplemented as shown below:

$$
\mathbf{D}_{1\mathrm{sx}} = \begin{bmatrix} \frac{c_{\mathrm{sx}}}{m_1} & \frac{d_{\mathrm{sx}}}{m_1}\\ -1 & 0 \end{bmatrix}, \qquad \mathbf{D}_{1\mathrm{ax}} = \begin{bmatrix} \frac{1}{m_1}\\ 0 \end{bmatrix}. \tag{5.10}
$$

Using such a system configuration it is required to measure the relative displacement $q_{1\mathrm{x}} - q_{\mathrm{sx}}$ of a seat suspension and the absolute velocity $\dot{q}_{1\mathrm{x}}$ of an isolated body. The actual suspension deflection is evaluated easily by a cable extension position sensor that measures a relative displacement between the isolated body $q_{1\mathrm{x}}$ and the input vibration q_{sx}. The absolute velocity $\dot{q}_{1\mathrm{x}}$ of a suspended body is obtained by integrating the acceleration signal which is measured by using a linear accelerometer. In this paper an analog integrator together with high-pass filtering (an electronic device developed at the Koszalin University of Technology) is employed in order to compute the velocity signal without any drifting effect.

Thus the measurement vector is given as follows:

$$
\mathbf{y}_{\mathrm{x}}(t) := [q_{1\mathrm{x}} - q_{\mathrm{sx}}, \dot{q}_{1\mathrm{x}}]^{\mathrm{T}}. \tag{5.11}
$$

The corresponding measurement equation is given as the following arrangement:

$$
\mathbf{y}_{\mathrm{x}}(t) = \mathbf{C}_{2\mathrm{x}}\mathbf{x}_{\mathrm{x}}(t) + \mathbf{D}_{2\mathrm{sx}}\mathbf{w}_{\mathrm{sx}}(t) + \mathbf{D}_{2\mathrm{ax}}F_{\mathrm{ax}}(t) \tag{5.12}
$$

together with the additional matrices:

$$\mathbf{C}_{2\mathrm{x}} = \begin{bmatrix} 1 & 0 & 0 & 0 & 0 & 0 \\ 0 & 1 & 0 & 0 & 0 & 0 \end{bmatrix}, \tag{5.13}$$

$$\mathbf{D}_{2\mathrm{sx}} = \begin{bmatrix} -1 & 0 \\ 0 & 0 \end{bmatrix}, \qquad \mathbf{D}_{2\mathrm{ax}} = \begin{bmatrix} 0 \\ 0 \end{bmatrix}. \tag{5.14}$$

According to the state feedback control problem (Eq. (4.14)), the desired active force is attained by applying the following control policy:

$$F_{\mathrm{ax}}(t) = \mathbf{K}_{\mathrm{x}}\mathbf{y}_{\mathrm{x}}(t) \tag{5.15}$$

where the output feedback gain vector $\mathbf{K}_{\mathrm{x}} = [k_{1\mathrm{x}}, k_{2\mathrm{x}}]$ includes the proportionality factor $k_{1\mathrm{x}}$ of the relative displacement feedback loop and the proportionality factor $k_{2\mathrm{x}}$ of the absolute velocity feedback loop.

5.2. Multi-criteria optimisation of the control parameters

The control parameters $x_{\mathrm{d1}} := k_{1\mathrm{x}}$ and $x_{\mathrm{d2}} := k_{2\mathrm{x}}$ are selected as the decision variables that influence the dynamical properties of the suspension system significantly. Therefore a vector of the decision variables is determined as follows:

$$\mathbf{x}_{\mathrm{d}} = [x_{\mathrm{d1}}, x_{\mathrm{d2}}]^{\mathrm{T}}. \tag{5.16}$$

Then the transmissibility factor $\mathrm{TFE}_{\mathrm{x}}$ is chosen as the primary optimisation criterion:

$$\min_{\mathbf{x}_{\mathrm{d}}} \ \mathrm{TFE}_{\mathrm{x}}(\mathbf{x}_{\mathrm{d}}). \tag{5.17}$$

The value of this criterion is expressed as a percentage ratio of the frequency-weighted acceleration measured at the seat surface to the frequency-weighted acceleration coming form the input vibration [18]. The frequency weightings based on [19] are employed to represent the varied human sensitivity to mechanical vibration at different frequency ranges.

The secondary optimisation criterion (suspension travel s_{tx}) is transferred to the non-linear inequality constraint as following:

$$s_{\mathrm{tx}}(\mathbf{x}_{\mathrm{d}}) \le s_{\mathrm{txj}} \tag{5.18}$$

where s_{txj} is the constraint value of suspension travel. Its value demonstrates the maximum deflection (rebound) of the suspension system relative to the seat base. Such an optimisation criterion should be also minimised in order to provide the desired contact with the driver's steering devices [20].

In this paper the concept of Pareto-optimality is implemented [21] and the optimisation procedure is carried out by applying random starting points that

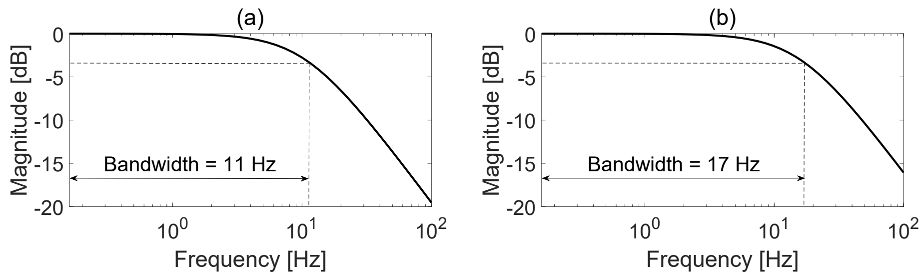

FIG. 6. Frequency response of the applied actuators: magneto-rheological damper (a), pneumatic muscles (b) and their corresponding frequency bandwidths.

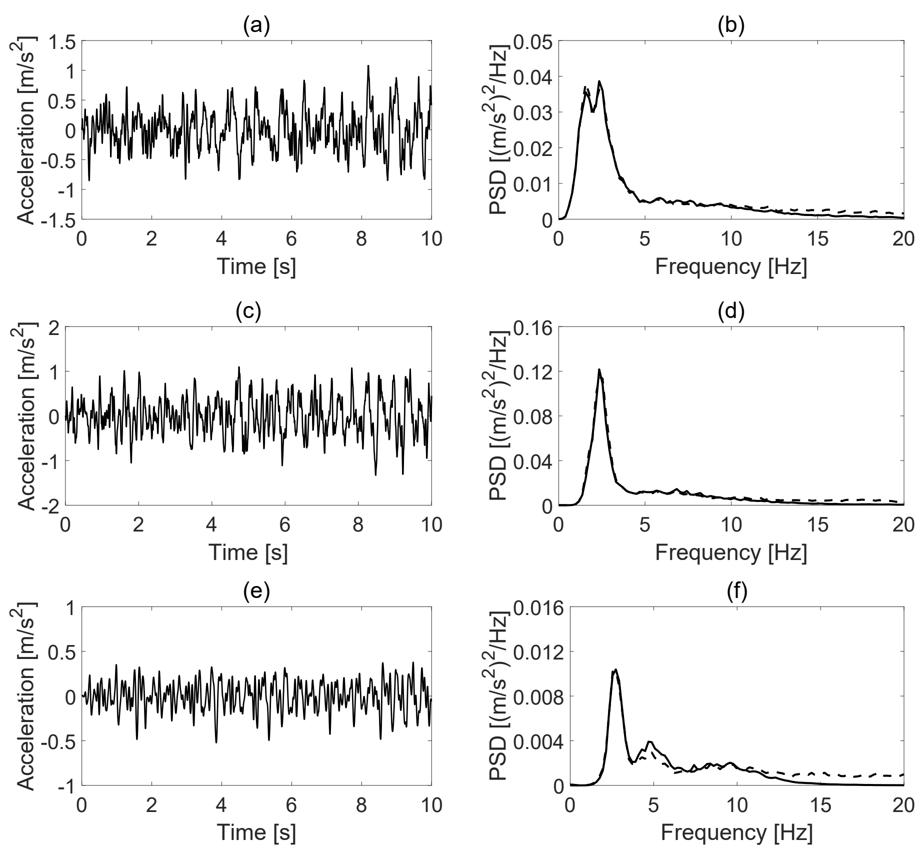

FIG. 7. Time histories of the acceleration input signals: AT1x (a), AT2x (c), RV1x (e), simulated (solid line) and measured (dashed line) power spectral densities of horizontal excitation signals: AT1x (b), AT2x (d), RV1x (f).

are generated within knowingly specified bounds of the decision variables. There are two actuation systems considered for vibration control of the seat, i.e. the magneto-rheological damper (semi-active suspension) and the pneumatic muscles (active suspension). Frequency responses of the applied actuators and their corresponding frequency bandwidths are shown in Fig. 6. A detailed description of the system modelling equations can be found in the Authors' previous papers [22, 23].

The vibro-isolation behaviour of semi-active and active suspension is selected individually for the following horizontal input vibrations that affect the drivers of different machinery at work:

- AT1x – agricultural tractor on road at speed 30 kph,
- AT2x – agricultural tractor on road at speed 40 kph,
- RV1x – rail vehicle.

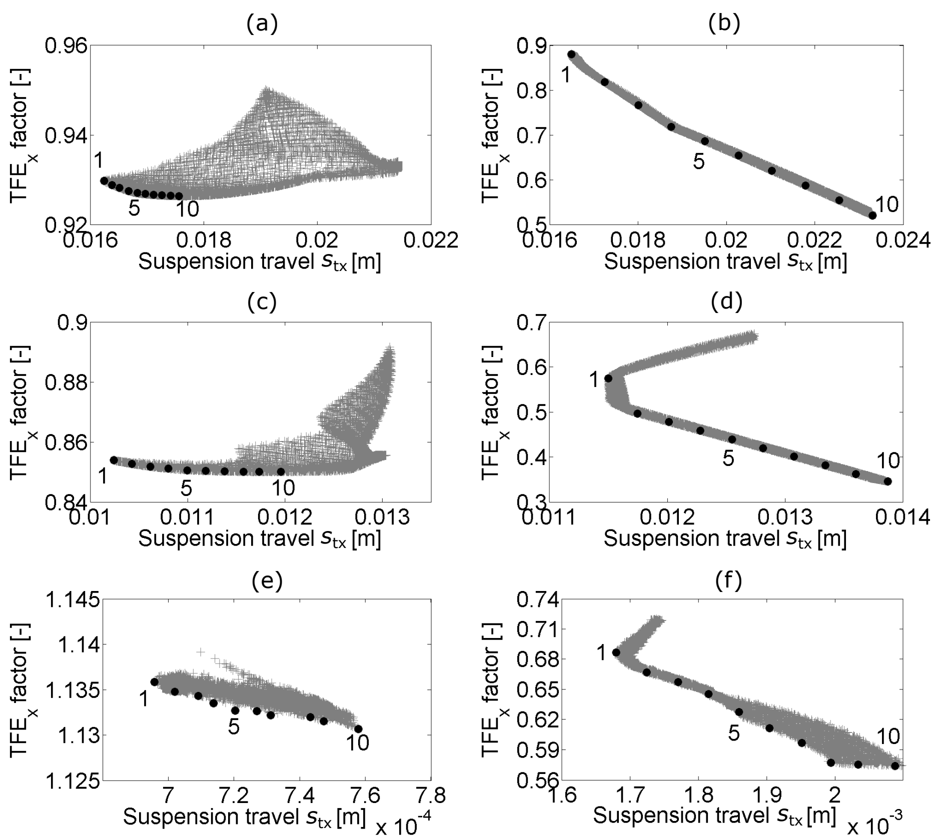

Fig. 8. Pareto-optimal point distribution (bullets) of semi-active system for the selected input vibration: AT1x (a), AT2x (c), RV1x (e) and active system for the selected input vibration: AT1x (b), AT2x (d), RV1x (f).

The test inputs listed above are measured as a part of the work that has been done by Isringhausen GmbH & CO. KG as well as established within the framework of the European research project VIBSEAT [24]. Time histories of the accelerations and corresponding power spectral densities of the mentioned horizontal input vibrations are shown in Fig. 7.

Ten Pareto-optimal system configurations are identified for the excitation signals with specific spectral characteristics. In Fig. 8 the Pareto-optimal point distribution of semi-active and active suspension systems is presented. The marginal solutions shown in this figure defines the extreme system configurations, i.e. the solution No. 1 indicates very stiff suspension, however the solution No. 10 designates very soft suspension. The solutions shown between points from No. 2 up to No. 9 establish compromising configurations of the seat suspension system. They are represented by a specific set of the decision variables that is assigned to the corresponding control parameters (see Figs. 9 and 10).

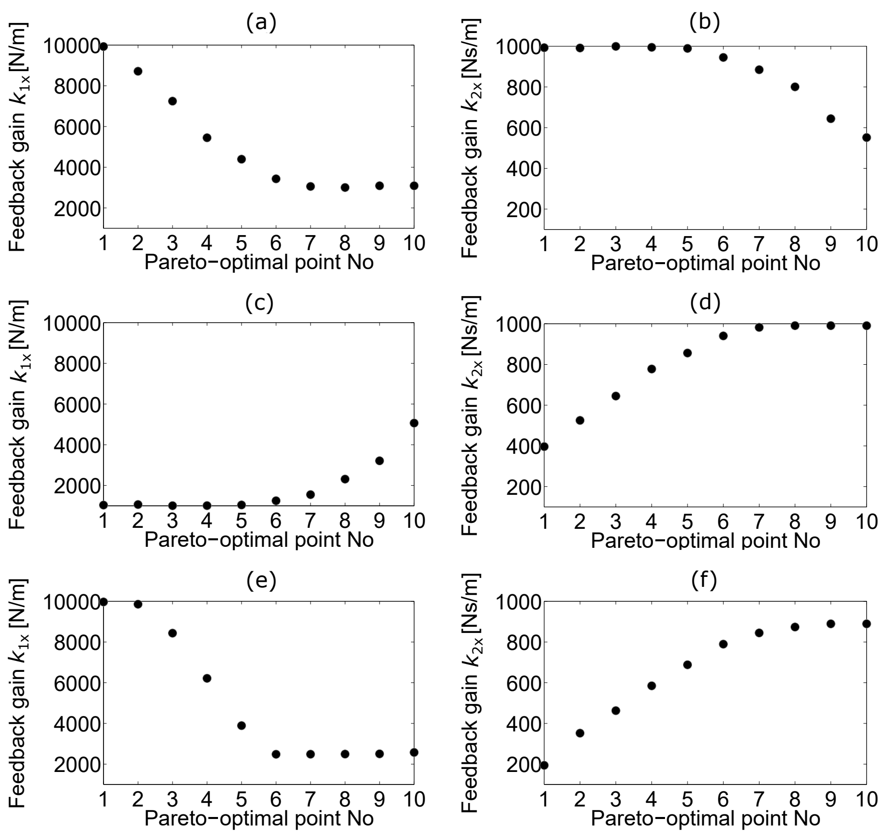

Fig. 9. Optimal control parameters of the semi-active suspension with MR damper obtained for the following input vibration: AT1x (a–b), AT2x (c–d), RV1x (e–f).

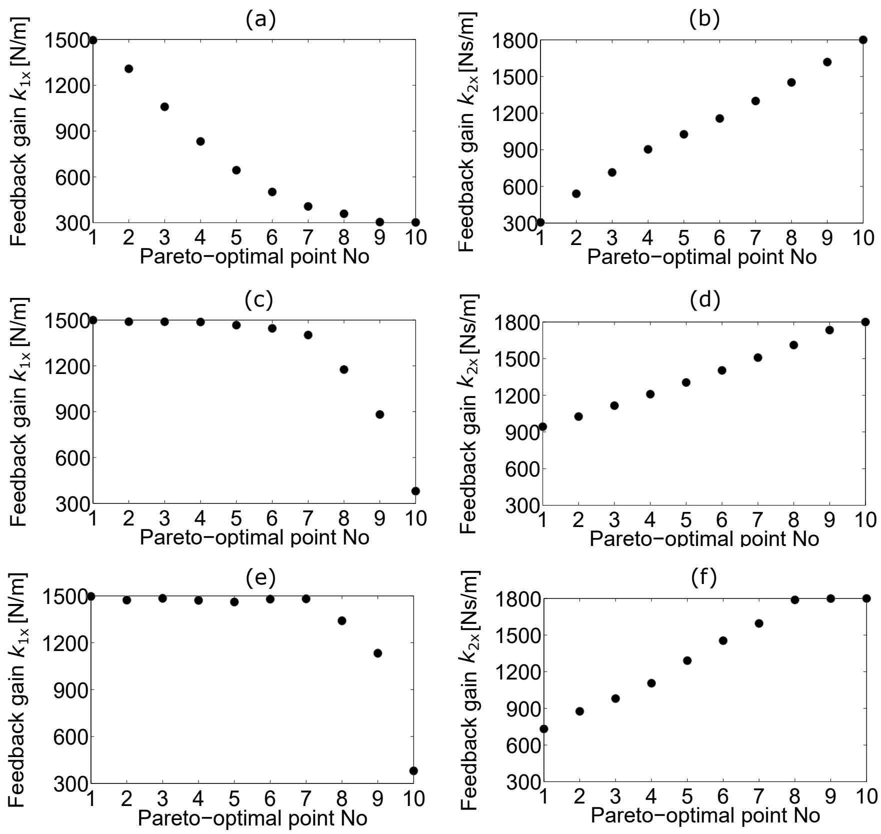

Fig. 10. Optimal control parameters of the active suspension with pneumatic muscles obtained for the following input vibration: AT1x (a–b), AT2x (c–d), RV1x (e–f).

5.3. Laboratory examination of the seat vibration control by using semi-active and active suspension system

The laboratory examination of the semi-active and active seat suspension is executed with the use of the NI cRIO-9074 embedded controller which is applicable for advanced control and monitoring applications. Such a hardware controller features a real-time processor that allows to implement control strategy by utilising a graphical programming language LabVIEW®. Using this controller sophisticated control algorithms are programmed for regulating the force of magnetorheological damper (semi-active system) as well as for adjusting the air pressure inside pneumatic muscles (an active system). Optimal values of the control parameters for semi-active (Fig. 9) and active seat suspension systems (Fig. 10) are included in the designed control policy that is optimised relative to the conflicted vibro-isolation criteria. In this paper the system configuration close to the Pareto-optimal solutions No. 10 is investigated experimentally for which the transmissibility factors $\mathrm{TFE_x}$ have the lowest values. The obtained suspension travels s_{tx} indicate acceptable ranges of the system relative displacements, therefore undesirable contact with the end-stop buffers may occur occasionally.

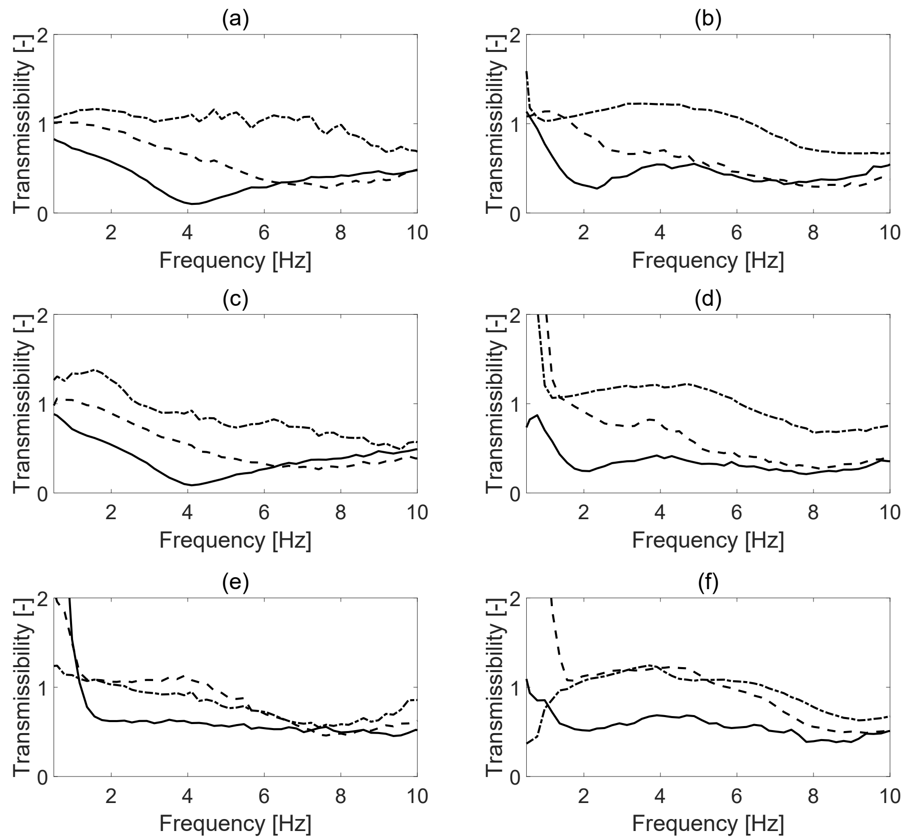

Fig. 11. Transmissibility functions of the passive (dash-dotted line), semi-active (dashed line) and active (solid line) horizontal seat suspension obtained by using simulation model for different spectral classes: AT1x (a), AT2x (c), RV1x (e) and measured experimentally for different spectral classes: AT1x (b), AT2x (d), RV1x (f), human body mass 90 kg.

Transmissibility functions of the passive, semi-active and active seat suspension for the particular input vibrations, i.e. AT1x, AT2x and RV1x are illustrated in Fig. 11. As shown in this figure, a satisfactory effectiveness of vibration reduction is noticeable almost in the whole frequency range of an excitation signal. Nonetheless, an amplification of the vibration amplitudes is observed for the semi-active seat suspension at rather low frequencies (below 1 Hz). This effect is caused by an insufficient force of the magneto-rheological damper when its cycling is relatively slow. In that frequency range the whole-body vibration are strongly reduced by means of the pneumatic muscles that are powerful enough to absorb the harmful vibration energy. It should be noted, that the transmissibility of over 2 at a low frequency range is caused by a lack of the input vibration (see Fig. 7). In order to evaluate the quality performance of the seat suspension system, the transmissibility function is used as a ratio of the isolated body vibration in relation to the input vibration. If the vibration amplitude of input signal is close to zero at low frequencies then the transmissibility function tends to infinity.

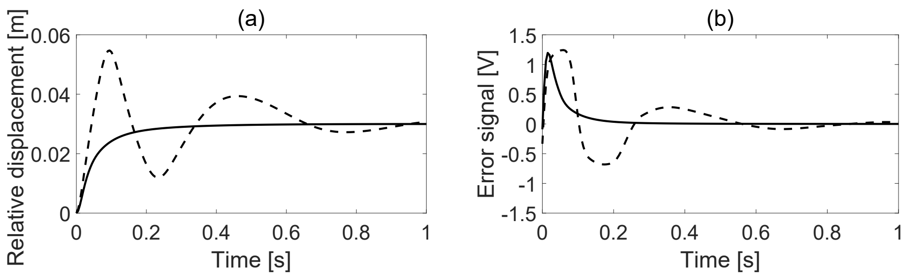

Fig. 12. Step response of the semi-active (dashed line) and active (solid line) horizontal seat suspension (a) and corresponding controller error with respect to time (b).

Although the comparison between control responses is shown in Fig. 11, the transmissibility functions alone do not show why the semi-active and active systems behave differently. The actuator dynamics play a significant role regarding the system effectiveness, therefore a step response of the semi-active and active horizontal seat suspension is considered in Fig. 12a. The corresponding controller error with respect to time is presented In Fig. 12b. As it is shown in both figures, the active system with pneumatic muscles is capable to attenuate vibrations much more efficiently than the semi-active system with MR damper. The time response of an active system is considerably shorter and the controller error is quickly eliminated by the proposed control strategy. The step response of semi-active system points out substantial oscillation around the set-point thus a meaningful overshoot is occurred by this kind of vibration control.

Table 1. Numerical values of the transmissibility factors and suspension travels obtained for excitation signals: AT1x, AT2x, RV1x, human body mass 90 kg.

	Passive		Semi-active		Active	
Input vibration	TFE_x factor	s_{tx}, mm	TFE_x factor	s_{tx}, mm	TFE_x factor	s_{tx}, mm
AT1x	1.104	5.3	0.922	17.2	0.521	23.3
AT2x	1.132	6.9	0.854	12.3	0.338	13.9
RV1x	1.107	0.2	1.129	0.7	0.564	2.1

The measurements results obtained for the human weight of 90 kg are compared in Table 1. As summarised in this table, the transmissibility factors TFE_x measured for the active suspension are lower of about 50% compared to the semi-active system. This clearly shows that the vibration damping effectiveness of the suspension system with pneumatic muscles is much higher than the system with magneto-rheological damper. Nevertheless, the active system requires a larger suspension stroke in order to efficiently reduce vibrations transmitted to the driver of different machinery.

6. Conclusions

This paper offers an original methodology for shaping the vibro-isolation properties of semi-active and active systems. Their dynamic characteristics may be consciously selected for a specific input vibration that adversely affects the human body at work. A generalised model of the human body effectively supports a control system synthesis for a single axis of the vibration transmission. Moreover, the multi-criteria optimisation can be successfully employed to find appropriate values of the control parameters in respect to conflicted vibro-isolation criteria. The vibro-isolation properties of semi-active and active vibration reduction systems are capable to be adjusted in accordance with the Pareto-optimal system configuration.

Acknowledgements

The paper is a part of the research project "Methods and procedures of selecting vibro-isolation properties of vibration reduction systems" founded by the National Science Center of Poland under the contract No. UMO-2013/11/B/ST8/03881. We would like to thank Isringhausen GMBH and CO. KG for the assistance in the experimental research.

References

1. I. Maciejewski, L. Meyer, T. Krzyzynski, *Modelling and multi-criteria optimisation of passive seat suspension vibro-isolating properties*, Journal of Sound and Vibration, **324**, 520–538, 2009, 10.1016/j.jsv.2009.02.021.

2. R.A. Ibrahim, *Recent advances in nonlinear passive vibration isolators*, Journal of Sound and Vibration, **314**, 371–452, 2008, 10.1016/j.jsv.2008.01.014.

3. B. Yan, M.J. Brennan, S.J. Elliott, N.S. Ferguson, *Active vibration isolation of a system with a distributed parameter isolator using absolute velocity feedback control*, Journal of Sound and Vibration, **329**, 1601–1614, 2010, 10.1016/j.jsv.2009.11.023.

4. T.S. Morais, J. Hagopian, V. Steffen, J. Mahfoud, *Modeling and identification of electromagnetic actuator for the control of rotating machinery*, Shock and Vibration, **20**, 171–179, 2013, 10.3233/SAV-2012-0735.

5. P.V.S. Sobhan, M.S. Rao, M.V. Sudarsan, D.M. Swamy, *Higher order sliding mode control of electromagnetic suspension system*, International Journal of Control Theory and Applications, **10**, 139–147, 2017.

6. G. Zhang, Y. Zhang, F. Yu, *Active suspension robust control based on main/torque-tracking loop structure*, Journal of Vibration and Control **19**, 1123–113, 2012, 10.1177/1077546312441656.

7. X. Su, X. Yang , P. Shi, L. Wu, *Fuzzy control of nonlinear electromagnetic suspension systems*, Mechatronics, **24**, 328–335, 2014, 10.1016/j.mechatronics.2013.08.002.

8. P. Hui, Ch. Ying, J.N. Chen, X. Liu, *Design of LQG controller for active suspension without considering road input signals*, Shock and Vibration, Article ID **6573567**, 1–13, 2017, 10.1155/2017/6573567.

9. H. Du, N. Zhang, *H-inf control of active vehicle suspensions with actuator time delay*, Journal of Sound and Vibration, **301**, 236–252, 2007, 10.1016/j.jsv.2006.09.022.

10. M. Gudarzi, A. Oveisi, *Robust control for ride comfort improvement of an active suspension system considering uncertain driver's biodynamics*, Journal of Low Frequency Noise, Vibration and Active Control, **33**, 317–339, 2014, 10.1260/0263-0923.33.3.317.

11. M. Maslanka, B. Sapinski, J. Snamina, *Experimental study of vibration control of a cable with an attached MR damper*, Journal of Theoretical and Applied Mechanics, **45**, 893–917, 2007.

12. S. Rutzel, B. Hinz, H.B. Wolfel, *Modal description – A better way of characterizing human vibration behavior*, Journal of Sound and Vibration, **298**, 810–823, 2006, 10.1016/j.jsv.2006.06.019.

13. G.J. Stein, P. Mucka, R. Chmurny, B. Hinz, R. Bluthner, *Measurement and modelling of x-direction apparent mass of the seated human body - cushioned seat system*, Journal of Biomechanics, **40**, 1493–1503, 2007, 10.1016/j.jbiomech.2006.06.012.

14. M. Toward, J. Griffin, *The transmission of vertical vibration through seats: Influence of the characteristics of the human body*, Journal of Sound and Vibration, **330**, 6526–6543, 2011, 10.1016/j.jsv.2011.07.033.

15. S. Yildirim, *Vibration control of suspension systems using a proposed neural network*, Journal of Sound and Vibration, **277**, 1059–1069, 2004, 10.1016/j.jsv.2003.09.057.

16. T. Yoshimura, K. Nakaminami, M. Kurimoto, J. Hino, *Active suspension of passenger cars using linear and fuzzy-logic controls*, Control Engineering Practice, **7**, 41–47, 1999, 10.1016/S0967-0661(98)00145-2.

17. D. Gu, P. Petkov, M. Konstantinov, *Robust Control Design with MATLAB*, Springer, Berlin, 2005, 10.1007/978-1-4471-4682-7.

18. G. Paddan, M. Griffi, *Use of Seating to Control Exposures to Whole-body Vibration*, Health and Safety Executive, London, 2001.

19. International Organization for Standardization, *Mechanical Vibration and Shock – Evolution of Human Exposure to Whole Body Vibration*, ISO 2631, Genewa, 1997.

20. A. Preumont, *Vibration Control of Active Structures An Introduction*, Springer, Berlin Heidelberg, 2011, 10.1007/978-94-007-2033-6.

21. I. Maciejewski, T. Kiczkowiak, T. Krzyzynski, *Application of the Pareto-optimal approach for selecting dynamic characteristics of seat suspension systems*, Vehicle System Dynamics, **49**, 1929–1950, 2011, 10.1080/00423114.2011.560270.

22. I. Maciejewski, S. Pecolt, Krzyzynski T, W. Markiewicz, *Controlling the vibration of a seat suspension system with the use of a magneto-rheological damper*, The Archives of Automotive Engineering, **77**, 59–69, 2017, 10.14669/AM.VOL77.ART6.

23. I. Maciejewski, T. Krzyzynski, H. Meyer, *Modeling and vibration control of an active horizontal seat suspension with pneumatic muscles*, Journal of Vibration and Control, Online First, 1–13, 2018, 10.1177/1077546318763435.

24. P. Clement, *Laboratory test protocol for assessing the vibration performance of seats equipped with horizontal suspensions*, Technical Report for the Competitive and Sustainable Growth Programme VIBSEAT G3RD-CT-2002-00827, **4**, 1–26, 2005.

Received October 30, 2018; revised version March 5, 2019.
Published online May 21, 2019.